To link to this article : DOI:10.1016/j.atmosres.2013.09.016
URL : http://dx.doi.org/10.1016/j.atmosres.2013.09.016

Analysis of flash flood-triggering rainfall for a process-oriented hydrological model

P.A. Garambois [a,b,*], K. Larnier [a,b], H. Roux [a,b], D. Labat [a,c], D. Dartus [a,b]

[a] Université de Toulouse, INPT, UPS, IMFT (Institut de Mécanique des Fluides de Toulouse), Allée Camille Soula, 31400 Toulouse, France
[b] CNRS, IMFT, 31400 Toulouse, France
[c] Géosciences Environnement Toulouse-Université de Toulouse-CNRS-IRD-OMP, 31400 Toulouse, France

A B S T R A C T

We propose an extended study of recent flood-triggering storms and resulting hydrological responses for catchments in the Pyrenean foothills up to the Aude region. For hydrometeorological sciences, it appears relevant to characterize flash floods and the storm that triggered them over various temporal and spatial scales. There are very few studies of extreme storm-caused floods in the literature covering the Mediterranean and highlighting, for example, the quickness and seasonality of this natural phenomenon. The present analysis is based on statistics that clarify the dependence between the spatial and temporal distributions of rainfall at catchment scale, catchment morphology and runoff response. Given the specific space and time scales of rainfall cell development, we show that the combined use of radar and a rain gauge network appears pertinent. Rainfall depth and intensity are found to be lower for catchments in the Pyrenean foothills than for the nearby Corbières or Montagne Noire regions. We highlight various hydrological behaviours and show that an increase in initial soil saturation tends to foster quicker catchment flood response times, of around 3 to 10 h. The hydrometeorological data set characterized in this paper constitutes a wealth of information to constrain a physics-based distributed model for regionalization purposes in the case of flash floods. Moreover, the use of diagnostic indices for rainfall distribution over catchment drainage networks highlights a unimodal trend in spatial temporal storm distributions for the entire flood dataset. Finally, it appears that floods in mountainous Pyrenean catchments are generally triggered by rainfall near the catchment outlet, where the topography is lower.

Keywords:
Flash floods
Rain gauge
Radar
Catchment
Rainfall characterization
Regionalization

1. Introduction: context of the issue

The proximity of the Mediterranean Sea and the steep surrounding topography can foster the lifting of low-level flow in an unstable atmosphere, as for the Alps and Pyrenees (Cohuet et al., 2011; Davolio et al., 2009; Riesco Martín et al., 2013). The mesoscale factors leading to convection in a variety of forms, ranging from shallow to deep convection, are still poorly understood (Tarolli et al., 2012). Nuissier et al. (2008) examined the synoptic conditions with low-level moist warm air flow for three torrential rainfall events in the South-East of France, and more specifically the Aude region near the Pyrenean foothills and the Gard region. In the latter, precipitation varies enormously both in time and space. A study of flash flood-generating storms in the Italian Alps revealed extreme spatial gradients up to 80 mm km^{-1} in accumulated precipitation over 12 h (Norbiato et al., 2007). The combination of great variability in rainfall distribution and heterogeneous catchment properties can make hydrological processes variable and difficult to predict. According to (Tarolli et al., 2012), the accurate characterization of flash floods and their regimes is an important aspect of climate and hydrometeorological science. The authors show differences in

* Corresponding author at: IMFT, allée du Pr. Camille Soula, 31400 Toulouse, France.
E-mail address: Pgarambo@Imft.Frc (P.A. Garambois).

storm coverage, seasonality and hydrological characteristics between the North-Western and South-Eastern Mediterranean regions.

The North-Western Mediterranean region is prone to heavy rainfall, especially in autumn, often triggering severe flash floods. They represent one of the most destructive hazards in this region and have caused billion of euros of damage over the last two decades (Gaume et al., 2004). Llasat et al. (2010) point out the high frequency and impact of flash floods in the North-Western Mediterranean region with vulnerable urbanized and densely populated areas. Moreover, the steepness of numerous small catchments (of a few km^2) favours rapid concentration times, and the generation of runoff can suddenly turn into devastating floods. Water depth in the drainage network can peak within a few minutes or a few hours, and flash flood prediction and risk assessment still lack efficient procedures, mainly because these events are poorly monitored and understood (Marchi et al., 2010). Characterizing the response of catchments to intense rainfall may provide new and valuable insights into the hydrological processes involved and their dependency on certain catchment properties (Archer et al., 2007; Borga et al., 2008; Delrieu et al., 2005).

Several studies on flash flood characterization in Europe can be found in the literature. Gaume et al. (2009) inventoried selected events across Europe for seven large regions of 90,000 km^2 on average over the last six decades and analysed flood peak distributions. They noted that in Mediterranean Europe, floods generally occur in autumn, and are more violent than continental European floods, which are most frequent in summer. Parajka et al. (2010) analysed the differences in long-term rainfall regimes using seasonality indices across the Alpine Carpathian range (more than 200,000 km^2). Marchi et al. (2010) studied 25 extreme flash floods (60 drainage basins ranging from 9.5 to 1856 km^2) across Europe. The authors checked the relationship between catchment area and flood response time, and estimated flood wave celerity in order to adapt monitoring network capacities.

These previous studies focused on extreme flash flood response for catchments ranging from a few square kilometres to several hundreds of square kilometres within quite large study regions of around 100,000 km^2.

We propose a study of flash floods and their generating storm on the scale of the Pyrenean foothills and the Aude region (10,000 km^2), within which we selected 11 small- to medium-sized catchment areas ranging from 36 to 776 km^2 with contrasting properties. This study stands astride meteorology and hydrology. We shall therefore discuss hydrological, geomorphological and meteorological aspects of flood genesis. The innovative aspects of this study are the consequential dataset gathered, despite the difficulties involved in monitoring flash floods, and the multidisciplinary approach applied. From a hydrological point of view and in order to predict flash floods on a regional scale, we analysed a catalogue of more than ten years of flood data representing a total of 60 flash floods. The analysis is based on statistics that clarify the relationship between spatial and temporal rainfall distribution at catchment scale, basin morphology and runoff response. Rainfall indices describe the overall spatial organization of rainfall in terms of geographical location and dispersion, in relation to flow distance to the catchment outlet. Better knowledge about the dependency of hydrological processes on catchment properties is useful for tailoring physics-based hydrological models to specific regions and predicting floods in ungauged areas.

The paper is organized as follows. Section 2 describes the study zone and the methodology applied to data collection. The physiographical properties of the 11 catchments studied are detailed in Section 3. Finally, Section 4 characterizes rainfall fields and related catchment flood responses.

2. Study zone and data collection

The aim of the data collection methodology proposed by Marchi et al. (2010) was threefold: (i) to identify the most possible flash floods in various (responding) catchments, (ii) to collect high-resolution flow and radar rainfall data enabling the characterization/modelling of flood response, initial soil moisture status, and (iii) to collect data on the morphological properties of each catchment area (digital elevation model – DEM – at 25-metre resolution, source: IGN, the French mapping and survey agency), land use (Corine Land Cover), soil properties and geology (Fig. 4).

Our selection of flood events was based not only on specific peak discharge, but other criteria such as storm duration and catchment size. Like (Gaume et al., 2009), we selected catchments of under 1000 km^2, but unlike them, we did not limit storm duration to 34 h. Indeed, some multiple peak flows or longer rain events are of interest when studying the behaviour of catchments. Of the systematically recorded flood and rainfall data for the last decade, we chose to study all the strongest flood responses with specific peak flow over 0.2 $m^3\ s^{-1} km^2$ for the selected catchments. The final catalogue for this study is composed of 11 catchments, representing a total of 60 flood events ranging from moderate flooding to major flash floods. Statistics are calculated for storm floods and indicate, for example, that three catchments respond simultaneously for a given storm (Table 1). The purpose is to analyse storm flood-generating mechanisms within a zone of a few hundred square kilometres. This data set contains flood events of different magnitudes. Thus, because of the variability of data, comments are often based on average statistics.

The literature contains several references about hydrological flood studies in the Spanish or French Pyrenees and related flood-prone areas (see, for example, (Gaume et al., 2004; Lajournade et al., 1998; Llasat et al., 2005)). The zone of interest for this paper is the eastern French Pyrenees, which is an area of particular interest for regional flash flood studies, providing a number of small to medium catchment areas (10–500 km^2) responding to the heavy rainfall frequent in this region. The Mediterranean climate zone is prone to heavy rainfall (Llasat et al., 2005; Molinié et al., 2011; Tramblay et al., 2011b) known as "cévenoles," often occurring with a South or South-East wind over the foothills of the

Table 1
General statistics of the 60 selected storm flood events.

	Min.	Max.	Average	Stdev.
Rainfall duration (h)	14	101	43	18
Cumulated rainfall (mm)	30	317	133	61
Number of responding catchments for a given storm	1	9	3	2
Lag time (h)	3	15	7	3

Alps, those of the Massif Central – the Cévennes – and of the Pyrenees (in this area, the Corbières. The mountainous topography plays an important role, at times blocking perturbations, which then regenerate and last several days. This was the case in September 2002 of the mesoscale convective system in the Gard region (Delrieu et al., 2005). We may also cite the widespread flooding of the Aude river in 1999, when 700 mm of rain fell within 24 hours (Bechtold and Bazile, 2001; Gaume et al., 2004). As an illustration, two hydrographs of important floods occurred on the Verdouble catchment in 1999 and 2005 are shown in Fig. 1. These are the two highest specific peak flows of 3 and 3.3 $m^3\ s^{-1}\ km^2$ within the dataset.

Our region of interest is located in South-West France along the Mediterranean coast. We selected 11 catchments in the eastern Pyrenean foothills with areas ranging from 36 to 776 km^2 (Table 2). A DEM data file of the study site with a grid scale of 25 m is available from IGN, the French mapping and survey agency (BD TOPO® © IGN – Paris – 2008. © (SCHAPI)).

Some of these catchments are tributaries of the Aude river that drains a mountainous area (Corbières) and flows through a narrow valley. Downstream from the city of Carcassonne, the morphology of the valley changes into a wide alluvial valley limited to the North by the relief of the Montagne Noire (North and North-East of Carcassonne) and to the South by the Corbières mountains. The Aude river has one main right-hand tributary (the Orbieu) which drains the northern part of the Corbières Mountains, and other smaller tributaries which drain the part of the Corbières Mountains further East (the Salz and Lauquet rivers). A succession of parallel tributaries join the Aude river along its left bank from the Montagne Noire (Fig. 2) (Gaume et al., 2004). We selected two left-hand tributaries from the Montagne Noire: the Orbiel and Cesse rivers, which cross the Canal du Midi before joining up with the Aude.

The southern part of the Corbières Mountains is drained by the Agly river and its main left-hand tributary, the Verdouble. Other small coastal rivers flowing into the sea near Perpignan, with very irregular flow regimes and contrasting characteristics, were also considered (Fig. 4): two steep catchments located in the Pyrenean mountains (the Tech and Têt river headwaters), and the Ballaury river, a small river that drains the Pyrenean foothills through steep vineyards near the sea and the French–Spanish border. The Réart river in the alluvial valley near Perpignan behaves like a wadi, with little water flowing in the superficial alluvial layer and sudden devastating floods.

Table 2
Catchment topography and flow length characteristics. The elevation ratio is the max–min elevation divided by the longest flow path.

Catchments	Area (km^2)	Altitude difference (m)	Maximal flow path length (km)	Relief ratio (m/m)
Tech	250	2730	34.5	0.079
Tet	776	2540	47.3	0.054
Réart	145	780	28.8	0.027
Verdouble	299	915	37.0	0.025
Agly	216	1640	33.5	0.049
Salz	144	995	17.2	0.058
Lauquet	173	795	29.1	0.027
Orbieu	263	840	37.6	0.022
Cesse	231	970	36.1	0.027
Orbiel	253	1200	34.8	0.034
Ballaury	36	890	10.4	0.086

3. Physiographical and drainage network characteristics

Physiographical factors can affect flash flood occurrence and characteristics in specific catchments by a combination of two main mechanisms: orographical influence on precipitation, and topographical effects promoting rapid concentration of stream flow (Costa, 1987; O'Connor and Costa, 2004). The flash flooding potential increases when a storm system remains over a fixed location for several hours, as was the case for the September 2002 flood event (Delrieu et al., 2005; Nuissier et al., 2008). A wide range of physical mechanisms, encompassing fluid dynamics, thermodynamics and cloud processes, in addition to larger-scale atmospheric circulation patterns, all influence precipitations. Instability, moisture and lifting are well known basic ingredients for convective storms, but the physical mechanisms that anchor

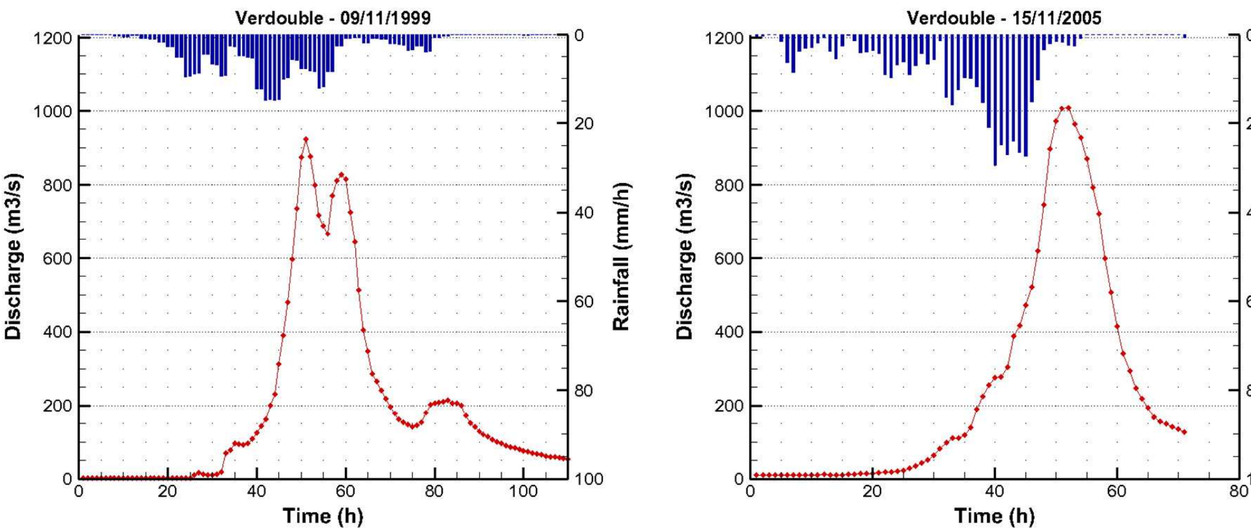

Fig. 1. Flash flood hydrographs for the Verdouble at Tautavel (299 km^2);(left) 09/11/1999 with rainfall from interpolated raingauges; (right) 15/11/2005 with radar rainfall.

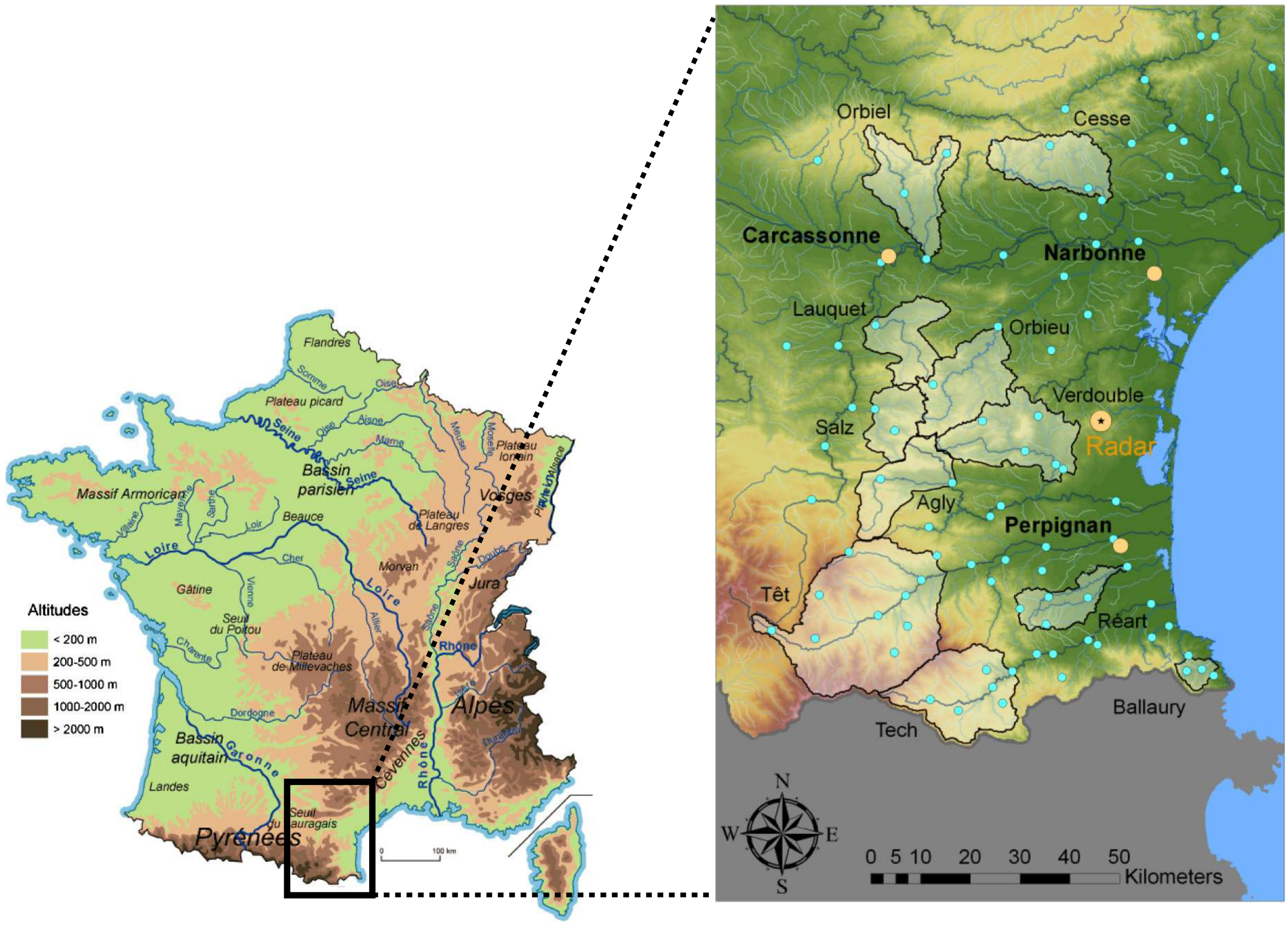

Fig. 2. (Left) Main Rivers and mountains of France. (Right) Study zone: Pyrenean foothills and Montagne Noire catchments, the Opoul radar (yellow starred circle), operational rain gauge network (blue dots), and main cities (yellow dots). (For interpretation of the references to colour in this figure legend, the reader is referred to the web version of this article.)

storms to a specific location are varied and often subtle. Moreover, it remains difficult to quantitatively measure or predict rainfall over complex terrain. We considered catchments with a marked topography of narrow valleys and steep hillslopes (Fig. 2). This relief channels runoff along the drainage flow pathways, resulting in high specific discharges and a significant geomorphic impact of flash flooding in catchment slopes.

The steepness of a basin is considered in terms of elevation distribution, with the hypsometric curve concept introduced by (Langbein, 1947), which shows the percent catchment area (area divided by total basin area) above a given percent elevation contour (Bras, 1990) (Fig. 3). Generally speaking, steepness decreases as the catchment area increases. From the Réart to the Têt, all the catchments have a strong topographical gradient. Moreover, the relief ratio – which is the height difference divided by the maximal flow path length – ranges between 0.022 and 0.086. When hillslope runoff occurs in quantity, these steep drainage networks can quickly lead to flood wave propagation.

Le Lay and Saulnier (2007) emit some hypotheses about the impact of the soil's spatial structure and hydraulic properties to explain several flash flood modelling results. Field studies in steep areas of the Cévennes region have also been undertaken to locally analyse runoff generation (Ayral, 2005). Based on hillslope infiltration experiments with either controlled rainfall inputs or real events, experimental results showed that the soil infiltration capacity is generally very high (more than 100 mm h^{-1}) and that a large portion of flow is generated by subsurface lateral paths.

In order to gain insight and propose a hypothesis about active processes controlling runoff generation, Manus et al. (2009) assessed the role of soil variability on runoff generation and catchment response during an extreme flash flood event (Gard 2002) (Delrieu et al., 2005). They proposed

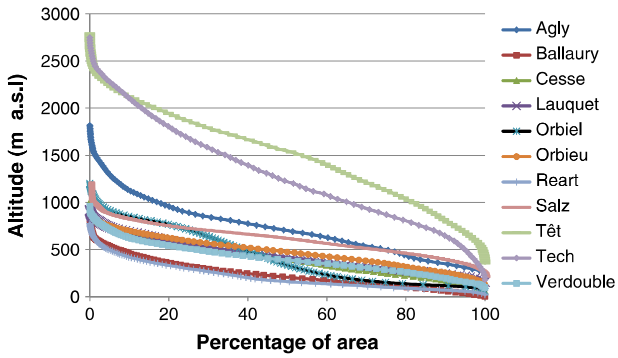

Fig. 3. Hypsometric curves, i.e. distribution curve of elevations per catchment.

a map distinguishing areas prone to saturation excess from those prone only to infiltration excess mechanisms. In accordance with the approach of (Manus et al., 2009) to rate the impact of soil variability on the hydrological response of small catchments, we extracted the soil's pedological characteristics from the Languedoc Roussillon soil database (referred to as BDSol-LR) provided by the INRA agronomy research institute (Robbez-Masson et al., 2002) (IGCS[1] software – BDSol-LR–version n° 2006, INRA – Montpellier SupAgro). We then applied the method explained in (Manus et al., 2009) to derive soil thickness maps (Fig. 3) from the wealth of information on superficial soil layers.

Braud et al. (2010) and Roux et al. (2011) both highlight the importance of soil thickness and texture on hydrological processes and catchment flood response. A comparative hydrological study recently showed that in Austria, flood response is significantly determined by geology (Gaál et al., 2012). In the Mediterranean region, geology and pedology are quite complex (Fig. 4), and bedrock faults or karst formations (Nou et al., 2011) can play a significant role in water balance, the first in water loss and the second in karst emptying triggered by a flood.

Land use is very varied in this study area, with moderate slopes occupied by vineyards in the Aude valley and tributaries, while the upper part of slopes is covered by scrubland. The central part of the Montagne Noire and the Pyrenees foothills is forested. The Aude watershed soils are mainly composed of silt and sand (Fig. 4). The dominant rock types are limestone and calciferous molasses. Locally, the limestone bedrock presents a high degree of karstification, especially in the Montagne Noire (Gaume et al., 2004; Nou et al., 2011). An examination of bedrock composition reveals huge differences between catchments, especially for the Tech and Têt with dominant granite and primary bedrock (Table 3). Four groups of catchments are defined in relation to bedrock similarity (Table 3). In our case, given the small catchment size and their proximity, the groups often correspond to neighbouring catchments on different sides or valleys of the same mountain.

4. Rainfall and flood characterization

In this section, we examine the characteristics of the rainfall that produced the flash flood with several statistics and indices. Statistics calculated from radar rainfall data give an idea of rainfall fields and catchment response characteristics that can help when critically analysing and understanding direct modelling results. Three catchment groups were defined on the basis of three geographical sub zones of the region of interest and more specifically to three distinct relief ensembles that might influence rainfall mechanisms (Table 4): Tech, Têt, Réart and Ballaury for the Pyrenees; Verdouble, Agly, Salz, Lauquet and Orbieu for the Corbières Mountains, and Cesse and Orbiel for the Montagne Noire area.

4.1. Rainfall and hydrometrical data

Fortunately, the French rain gauge and radar network coverage is relatively dense and offers useful data on storm event variability (Fig. 2). We have at least three operational rain gauges for the smallest catchment and seven for the largest (Têt), with records dating back decades. This operational rain gauge network is that of the SPCMO,[2] the regional flood forecasting service of the West Mediterranean region. We also used the water depth records and rating curves provided by SPCMO to calculate flood hydrographs at catchment outlets. The resolution of discharge data ranges from five minutes to an hourly time interval.

The required temporal resolution for flash flood monitoring is between 10 and 15 min with a rain gauge density of 1 per 20–35 km^2. The spatial resolution recommended by Sangati et al. (2009) is 2 km for correct quantitative radar rainfall estimation in order to simulate three extreme flash floods on the Sesia catchment in northern Italy. For this study, we used operational rain gauge-calibrated radar rainfall data at 5 min intervals and 1 km spatial resolution. Radar rainfall measurements by the Opoul radar (Fig. 2) are available from 2002. This radar belongs to the French operational radar network ARAMIS of Météo France that has developed good expertise and algorithms for rainfall estimation from radar reflectivity (Tabary, 2007; Tabary et al., 2007).

4.2. Flood-generating rainfall: amount and duration

A quantitative precipitation estimation gives access to rainfall intensity and distribution, influencing soil saturation and runoff dynamics when combined with local topography. Fig. 5 shows the relation between total event rainfall versus duration for the different catchments and floods considered in this study. Cumulative rainfall ranges from 30 mm in 26 h to 317 mm in 55 h (Cesse at Bize Minervois). The two Montagne Noire catchments (Set 3, Fig. 5) are subjected to the most intense rainfalls on average, with 154 mm in 34 h. The Corbières Mountain catchments (Set 2, Fig. 5) have similar cumulated rainfall on average, with 148 mm but over a period of 47 h. Set 1 (Fig. 5) – catchments in the Pyrenean foothills – is affected by an average rainfall of 93 mm over 43 h. The spread of the data set might indicate more or less intense and/or localized rainfall events.

Moreover, given the catchment areas we selected, Fig. 6 shows that rainfall develops at temporal scales within the detection capacity of both the rain gauge and radar networks, as shown by (Borga et al., 2008). Thus, the use of both radar and rain gauge rainfall data might be pertinent. It should be noted that rain gauge density within a catchment determines rainfall sampling, which is why radar rainfall data are used in this paper.

4.3. Unit peak discharge

Peak discharge is a helpful criterion for characterizing flood magnitude and its dependence on watershed area is widely accepted, as the body of literature can attest. One example is the relationship between discharge and catchment area both for single-event peak flow and mean annual peak flow ((Furey and Gupta, 2005; Gupta et al., 1996; Marchi et al., 2010) among

[1] http://gissol.orleans.inra.fr/.

[2] "Service de Prévision des Crues Méditerranée Ouest". Regional flood forecast service for the Languedoc Roussillon region.

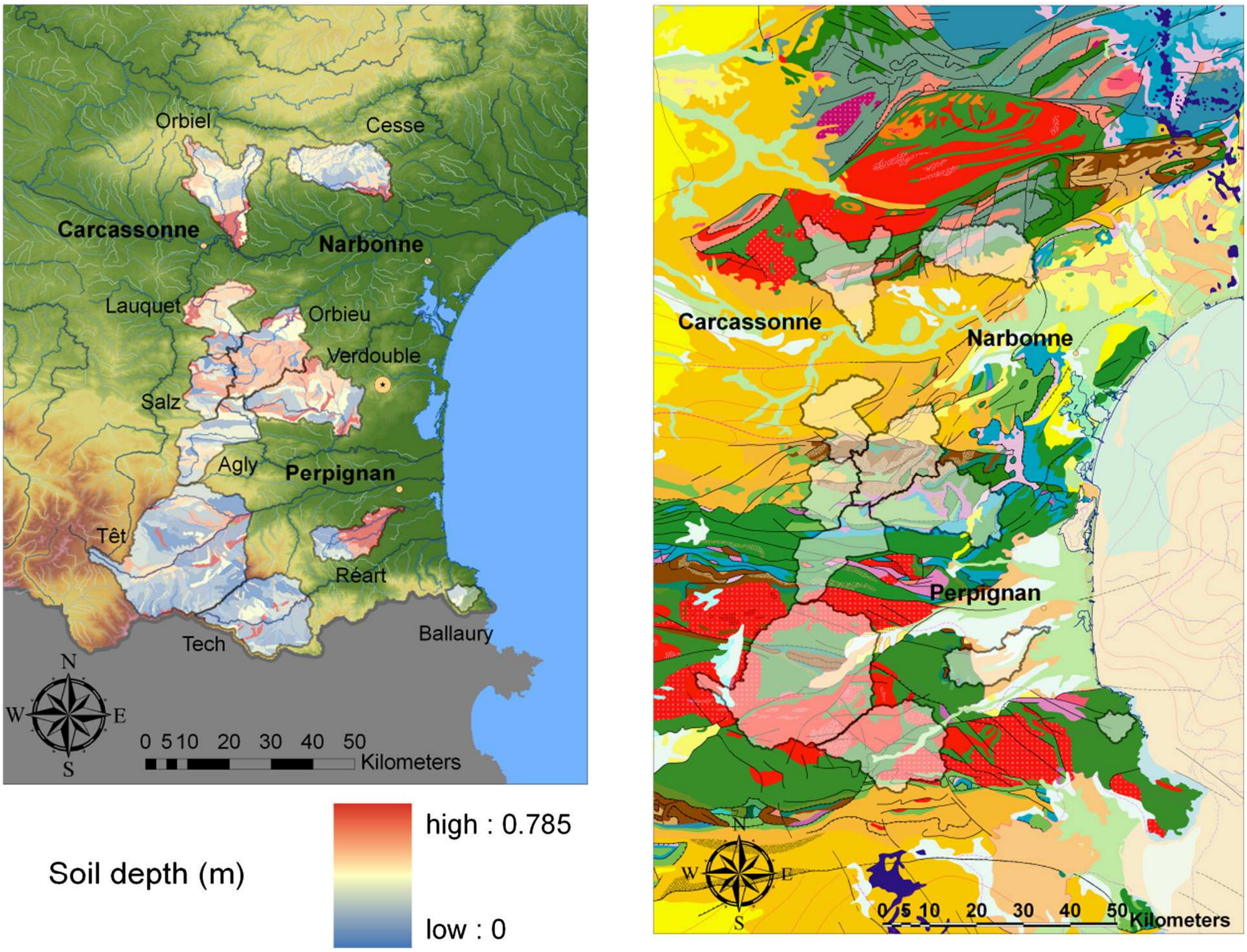

Fig. 4. (left) soil depth map (source BD-sols Languedoc Roussillon, INRA), (right) Geological formations and faults, large structural and lithological ensembles (Table 3) (source BD Million-Geol, BRGM).

Table 3
Catchment geology and colour correspondence for the lithology map (Fig. 4).

Catchments	Geology	Representation (Fig. 4, right)
Tech, Têt	- Granites and primary era formations (mainly schist but locally highly karstified limestone)	- Red, purple, brown and dark green
Verdouble, Agly, Ballaury	- Granites and primary era formation, (top right Verdouble and bottom left Agly on the map) -Mesozoic mainly cretaceous formations (limestone, marls)	- Red, purple, brown and dark green - Dark green, light green, turquoise, pink
Salz, Lauquet, Orbieu	- Primary era formations - Mesozoic, mainly cretaceous formations, - Tertiary era detritic formations (sands, molasses, conglomerates) - Quaternary alluvions	- Brown, light brown, dark green, purple - Green, turquoise - Orange, yellow - Light green, white
Cesse, Orbiel	- Granites and primary era formations (mainly schist but locally highly karstified limestones) - Tertiary era detritic formations (sands, molasses, conglomerates)	- Red, purple, brown and dark green - Orange, yellow

others). We consider specific peak discharge, i.e. maximal peak discharge normalized by catchment area (Fig. 7). Our results show that the events considered in this study are not as extreme as those considered for example by (Gaume et al., 2009; Herschy, 2002), who propose similar envelopes for the extreme flash flood discharges in Europe. The unit peak discharges reported range from 0.1 to 3 $m^3\ s^{-1}\ km^2$.

Note that the data set contains the worst floods of the last decade for most of these catchments, including devastating floods like the one in November 1999. Moreover, as highlighted by (Marchi et al., 2010), it is worth recalling that areas of moderate unit peak flows do not necessarily equate to areas of moderate flood risk, since the flood risk for any particular location is in part due to the local forecasting, warning and communication system, existing flood protection works, as

Table 4
Catchment groups for statistical analysis.

Group	Catchments
Catchment Set 1	Tech, Têt, Réart, Ballaury
Catchment Set 2	Verdouble, Agly, Salz, Lauquet and Orbieu
Catchment Set 3	Cesse, Orbiel

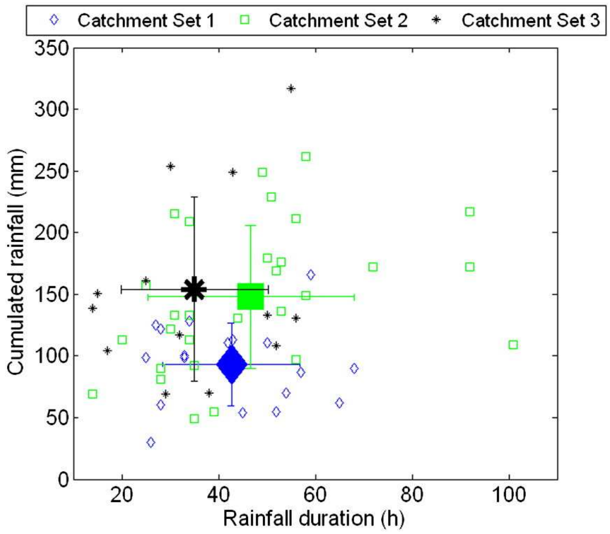

Fig. 5. Rainstorm duration versus cumulated rainfall. The big symbol represents the mean value for each catchment group, with standard deviation bars visible.

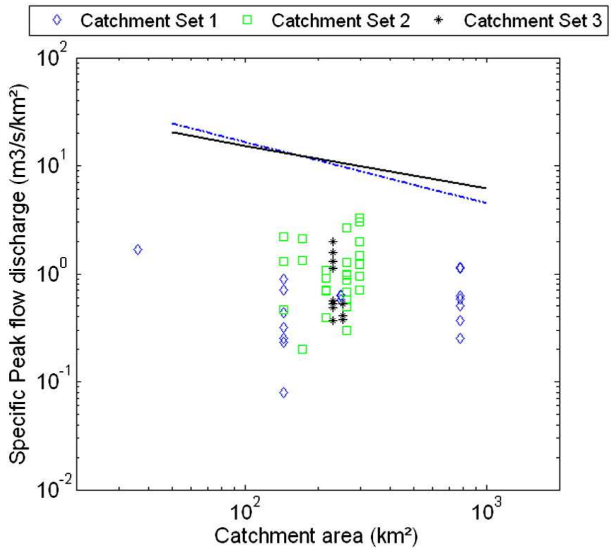

Fig. 7. Unit peak discharge of flood responses versus drainage area. The black and blue lines correspond to empirical power laws derived from the most extreme floods recorded in Europe (black solid line: ($Q_u = 97 * A^{-0.4}$) (Gaume et al., 2009), blue dash-dot line ($Q_u = 230 * A^{-0.57}$) (Herschy, 2002)). (For interpretation of the references to colour in this figure legend, the reader is referred to the web version of this article.)

well as the community's social, political, and regulatory setting. The Aude basin, which is quite flat and whose lower part is prone to flooding, is a quite densely populated region where flood risk is rooted in the collective conscience. We believe that for flood forecasting purposes, it is important to build a robust model and configure it such that it is not based on extreme events for which there are major uncertainties on rainfall and peak flow. The aim is to validate the model efficiently and forecast the order of magnitude of large floods.

4.4. Response time to atmospheric forcing

The specific problem of flash flood risk management is that these floods interact with social organization at space and time scales that imply unusually short warning lead times (Creutin et al., 2009). In order to estimate the response time, we used the concept (Dingman, 2002) of lag time in the following. We defined lag time as the duration between the centroid of rainfall and the peak time. We related the event lag time to morphological parameters and soil saturation conditions, because for different soil moisture conditions, the same rainfall does not result in comparable runoff generation. The lag time integrates flow velocity determined by the slopes, the amount of water and hydraulic friction. It also integrates the effects of

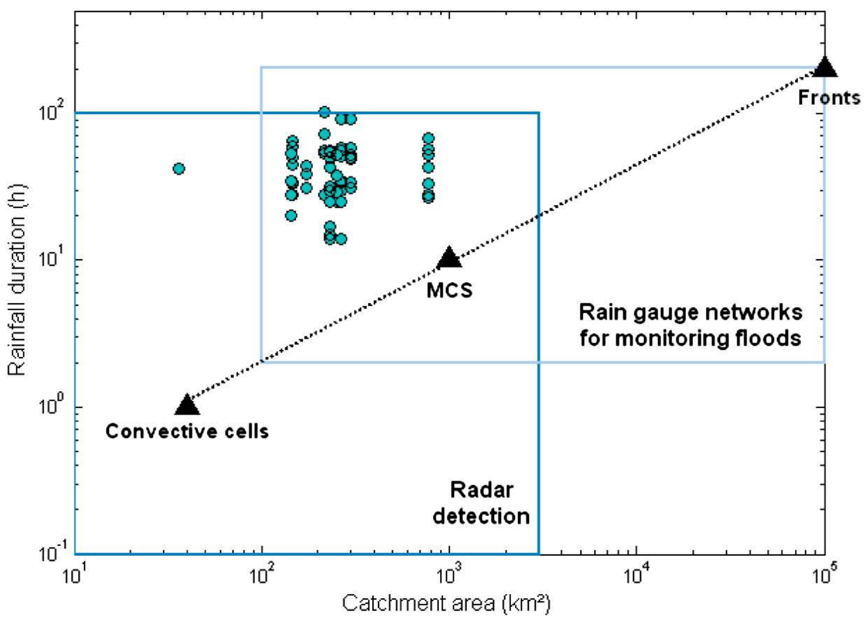

Fig. 6. Spatial temporal scales for the selected flash floods. Scales of convective cells and Mesoscale Convective Systems (MCS) are taken from (Orlanski, 1975). (Dark blue) radar detection and (light blue) rain gauge network monitoring capacities for flash flood-triggering rainfall are taken from (Borga et al., 2008). (For interpretation of the references to colour in this figure legend, the reader is referred to the web version of this article.)

rainfall distribution for a given catchment. The relationship to the catchment area is unclear, partly because we lacked catchments between 40 and 100 km^2 (Fig. 8, left).

Soil moisture is an important factor in Mediterranean flood genesis (Roux et al., 2011). We therefore used an initial soil moisture value for superficial layers estimated from a continuous operational water balance model run over the whole country using 8 km by 8 km cells. SAFRAN-ISBA-MODCOU (Habets et al., 2008) proved to be a good predictor of soil moisture conditions(Tramblay et al., 2011a). The large scatter in (Fig. 8, right) results from catchment flood response depending on the space-time interactions between rainfall, runoff generation and routing mechanisms (Viglione et al., 2010; Woods and Sivapalan, 1999). This illustrates the non stationarity and marked non linearity of the process determined by the combination of rainfall and catchment variability. It can be seen that the higher the initial soil saturation value, the quicker the catchment response. For initial saturation over 60%, the response time of the catchments considered is between three and ten hours.

4.5. Runoff coefficient

Runoff coefficient is a widely used concept in hydrology and an important diagnostic variable of runoff generation and catchment response. It is useful to examine runoff coefficients to compare catchments at different time scales in order to understand the dampening effect on rainfall of different landscapes. For flood-based runoff, specific questions concern: (i) quantification of runoff coefficients and analysis of possible regional differences (climatic, litho-pedological differentiation) (ii) relations with indicators of previous moisture for example. Event runoff coefficients are usually estimated as the ratio of event volume to event rainfall volume. They are calculated with an event hydrograph defined from the beginning of the hydrograph's rising limb to the end of event runoff. The time corresponding to event runoff was determined by separating the recession curve into surface and subsurface flow with semi-logarithmic diagrams (Tallaksen, 1995). Indeed, these two components are supposed to be characterized by different residence times within a catchment, surface runoff being quicker than subsurface flow. Moreover, for the catchments we studied, surface runoff is easily identified, with a generally low ratio of base flow to peak flow and quick recession. The runoff coefficients calculated that way range from 0.15 to 0.8, the mean value being 0.4 with a standard deviation of 0.17. This is the order of magnitude for Mediterranean catchments with relatively high runoff coefficients.

The relation between event runoff coefficient and event cumulated rainfall or initial soil saturation state is reported in (Fig. 9, left). Set 1 differs from Sets 2 and 3 by lower cumulated rainfall as stated before and lower runoff coefficients. Sets 2 and 3 are quite similar on average, but not as regards scatter (Fig. 9, standard deviation bars). Overall, the dependence is slight and the scatter large, with runoff coefficients spread over a wide interval within the range of precipitation depth and initial saturation state. There are several possible explanations for the wide scatter reported in (Fig. 9). Considering the meteorological factors for flash flood events generated by the prevailing mechanisms generating infiltration excess runoff, the runoff coefficient's magnitude may be more likely determined by the rainfall intensity rather than rainfall depth. A further potential source of scatter is the variability of initial soil moisture conditions which are combined with the subsurface water storage capacity to determine the amount of water input that can be stored and saturation dynamics. Several studies have highlighted the huge impact of soil moisture conditions on runoff for floods to extreme flash floods (Braud et al., 2010; Gaume et al., 2004; Tramblay et al., 2011a). Another source of scatter may be due to an error in the quantitative estimation of rainfall, which can be significant for these cases.

Fig. 9 (right), representing event runoff coefficient in relation to soil moisture, shows a mean event moisture of 57% at the beginning of the flood events considered, which range from 37% to 69%. It is interesting to remark that Set 1 shows

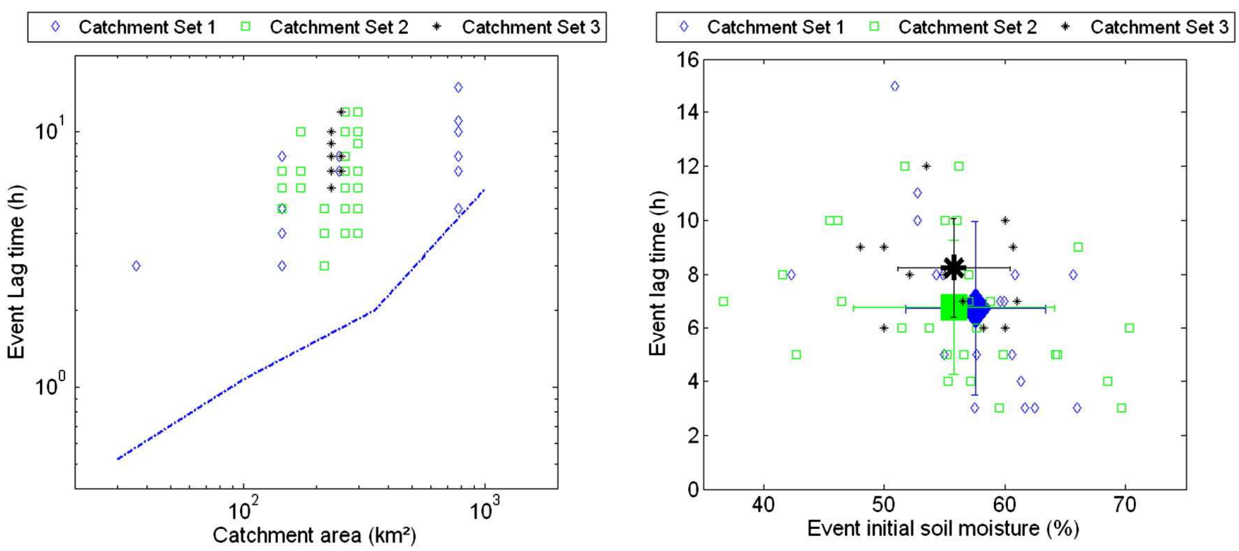

Fig. 8. Lag time versus catchment area (left). The blue line represents the empirical power law for the lower limit of catchment lag time (Robinson and Sivapalan, 1997); lag time versus initial soil moisture (right), with standard deviation bars visible. (For interpretation of the references to colour in this figure legend, the reader is referred to the web version of this article.)

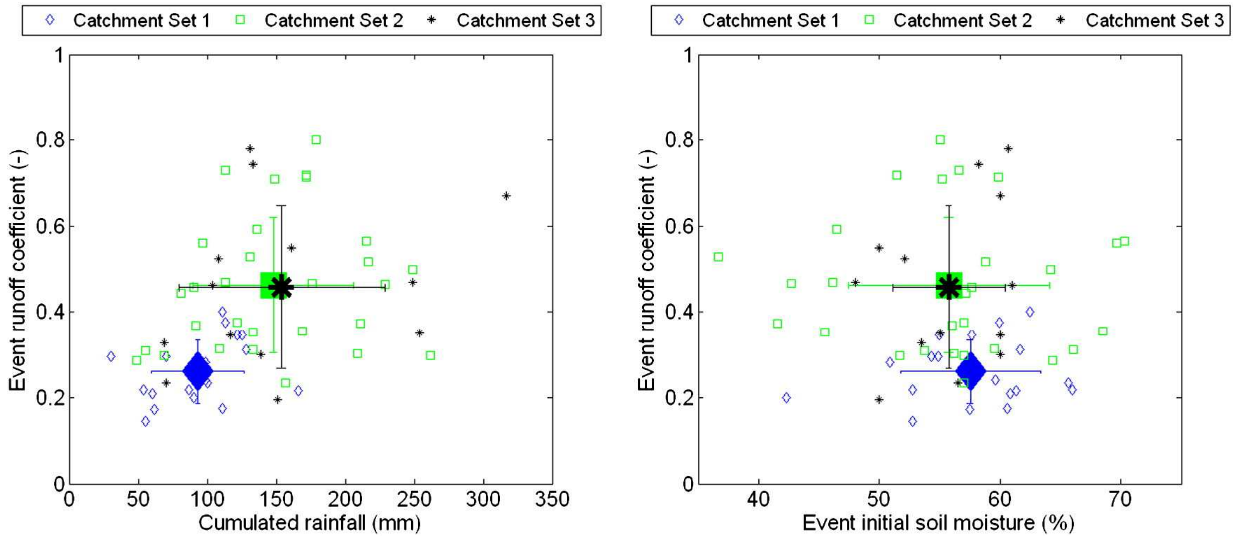

Fig. 9. Event runoff coefficient versus cumulated event rainfall (left). Event runoff coefficient versus initial soil water content (right); standard deviation bars are added.

lower runoff coefficients than the other catchments even for similar cumulated rainfall and initial soil saturation state. This can reveal non negligible differences in rainfall to runoff conservation, for example because of soil storage capacity or even bedrock percolation. Some Set 1 catchments might be influenced by specific litho-pedological properties, such as the Tech and Têt catchments whose substrate is developed mainly on granite and schist (Table 3 and Fig. 4 right). The entire dataset shows a huge variability in soil thickness and bedrock properties (Fig. 4). A comparison with response characteristics suggests that these catchments and floods represent a broad panel of hydrological behaviours, with non-linear processes concurring in time and space which require the use of a suitable model in order to help improve understanding.

4.6. Rainfall distribution by catchments

As stated before, catchment flood response dynamics and amplitude are sensitive to the resonance between the spatial temporal distribution of rainfall and catchment properties. (Woods and Sivapalan, 1999) outlined an analytical framework that quantifies the effects of space time variability on catchment storm response. The method proposed by (Smith et al., 2004) was extended by (Zoccatelli et al., 2010) for three flood events in the Carpathian range in Romania. The authors computed spatial and temporal rainfall statistics based on hydraulic routing distances. They showed that rainfall organization measured along the river network is a significant property of rainfall variability when considering flood response modelling. The formalism proposed in (Zoccatelli et al., 2011) provides useful information on what space time scale monitoring is required depending on catchment and flood characteristics.

Given the spatial rainfall data r(x,y,t) (L) on each pixel distant by d(x,y) (L) from catchment outlet, rainfall moments p_n (L^{n+1} T^{-1}) can be written:

$$p_n(t) = \frac{1}{A}\int_A r(x,y,t).d(x,y)^n dA \qquad (4-1)$$

With the catchment area A (L^2), the 0 order moment gives the mean rainfall intensity. Similarly, catchment moments g_n (L^n) in terms of distance to the outlet are written:

$$g_n = \frac{1}{A}\int_A d(x,y)^n dA \qquad (4-2)$$

And dimensionless moments of catchment rainfall are written:

$$\delta_1(t) = \frac{p_1(t)}{p_0(t).g_1} \qquad (4-3)$$

$$\delta_2(t) = \frac{\frac{1}{A}\int_A r(x,y,t).[d(x,y)\text{-}\delta_1(t)g_1]^2 dA}{\frac{1}{A^2}\int_A r(x,y,t).dA \times \int_A [d(x,y)\text{-}g_1]^2.dA} = \frac{1}{g_2\text{-}{g_1}^2}\left[\frac{p_2(t)}{p_0(t)}\text{-}\left(\frac{p_1(t)}{p_0(t)}\right)^2\right] \qquad (4-4)$$

According to (Zoccatelli et al., 2011), the first order moment δ1 (−) describes the distance of the centroid of catchment rainfall with respect to the average value of the flow distance (i.e. the catchment centroid). A value close to 1 reflects either spatially homogeneous rainfall or rainfall concentrated close to the catchment centroid. Values below one indicate that rainfall is near the catchment outlet, while values over one indicate rainfall toward the catchment headwaters.

The second scaled moment (4-4) describes the dispersion of rainfall. Values close to one reflect fairly uniform rainfall, whereas values below one mean that rainfall has a unimodal distribution along the flow distance.

We use these statistics to describe rainfall over storm duration T_S, with:

$$P_n = \frac{1}{A}\int_A r_t(x,y).d(x,y,t)^n dA = \frac{1}{T_S}\int_{T_S} p_n(t)dt \qquad (4-5)$$

where $r_t(x,y)$ is the time-integrated value of rainfall at location (x,y). The time-integrated moments thus become:

$$\Delta_1 = \frac{P_1}{P_0 \cdot g_1} \qquad (4-6)$$

$$\Delta_2 = \frac{1}{g_2 - {g_1}^2}\left[\frac{P_2}{P_0} - \left(\frac{P_1}{P_0}\right)^2\right] \qquad (4-7)$$

We calculated these indices for the entire flood event set. The mean value of Δ_1 is 0.97 with a standard deviation of 0.09, so the rainfall centroid must be close to the catchment centroid or spatially uniform. The mean value of Δ_2 is 0.83 and the standard deviation 0.15, which indicates on average a unimodal distribution of rainfall along the flow distance. This is the case for all three catchment sets, with a Δ_2 value around 0.83 (Fig. 10, right).

Fig. 10, left, shows a mean Δ_1 below one and a rather large error bar for Set 1. Flood-triggering rainfall events are therefore often located near the outlet for these catchments. In other words, rain falls on the lowest part of these catchments, whose difference in altitude can be over 2500 m. Rainfall is concentrated near the catchment centroid for Set 2 and Set 3 as Δ_1 is close to one. This could be due to a catchment size below 300 km^2, at least for sets 2 and 3, which appear to be less sensitive to large, quickly-moving rainfall cells.

Unsurprisingly, Fig. 10, right, does not show a particular tendency, given the number of non-linear processes involved in the rainfall to runoff transformation. It is thus difficult to explain hydrographical characteristics with a single variable characterizing the input. However, these indices could bring useful insights when analysed with distributed model outputs such as spatial maps of soil saturation to study the resonance of rainfall and catchment variability, or determine flood-prone areas within a catchment. Moreover, these indices reveal the sensitivity of small catchments to rainfall spreading as the variety of runoff coefficients found for different Δ_2.

5. Conclusion

We examined high-resolution data for 60 flash floods in the last decade that occurred in 11 headwater catchments of the eastern Pyrenean foothills covering areas ranging from 36 to 776 km^2. They proved to be interesting sites for studying the mechanisms behind flash floods given the quantity of static, meteorological and hydrometrical data available and the contrasting physical properties and behaviours. We summarize below the main results of this study for steep catchments with an elevation ratio ranging from 0.022 to 0.086 (m/m) and different litho-pedological properties. Significant variations were found for flood-triggering rainfall events at the scale of a few hundred kilometres in the Aude region.

- Rainfall depth and intensities are lower for the catchments of the Pyrenean foothills than for the nearby Corbières or Montagne Noire regions. Several floods in our data set were triggered by rainfall that generally hit the Montagne Noire and the Corbières mountains first and hardest before moving on to the Pyrenean foothills with relatively lower rainfall.
- We show that the use of both radar and the rain gauge network is pertinent for our data set, composed of medium floods to severe flash floods, given the space and time scales at which flood-triggering rainfall develops.
- The spreading of event runoff coefficients highlights the wide range of hydrological behaviour with non-linear processes concurring in time and space. High initial soil saturation levels tend to promote quicker catchment flood response times of some 3 to10 hours.
- The contrasting hydrological behaviour of the catchments considered requires the use of a suitable model in order to improve our understanding of flash flood dynamics.
- A robust model with appropriate parameterization is required for flood forecasting and regionalization, not based on extreme events for which there are major uncertainties as to rainfall and peak flow. The high-resolution data presented in this paper constitute a wealth of information with which to constrain a physics-based distributed model such as MARINE (Roux et al., 2011) for regionalization purposes.
- Scaled rainfall indices of rainfall distribution along a catchment drainage network reveal a unimodal trend in spatial temporal storm properties for the entire flood dataset. Moreover, it appears that the floods in the Pyrenean mountain catchments are generally triggered by rainfall near the outlet, where the topography is lower.

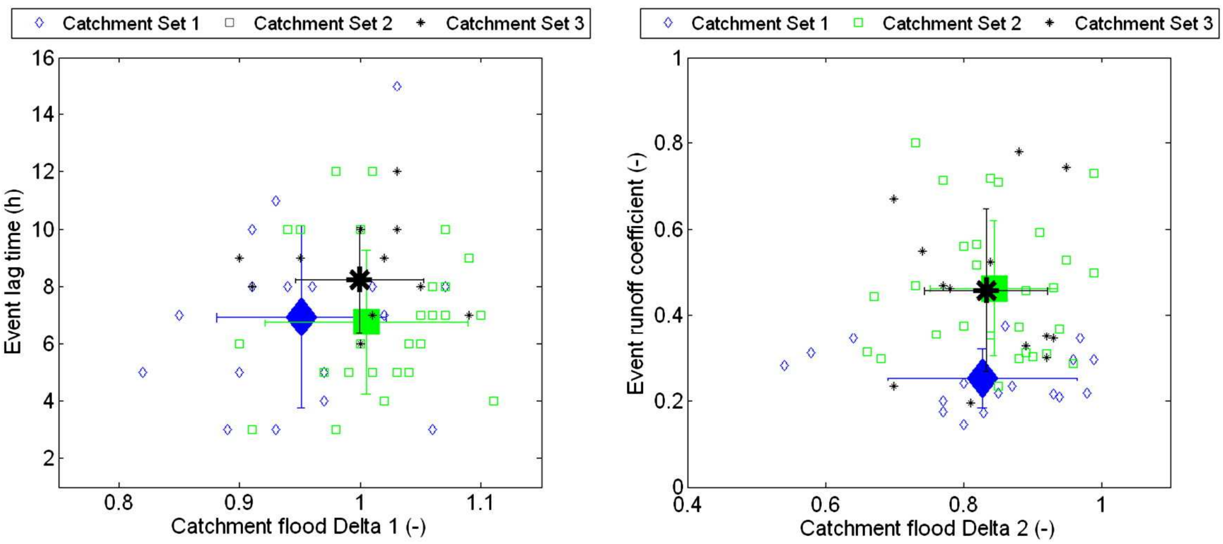

Fig. 10. (left) Event lag time related to Event catchment flood Δ_1; (right) Event runoff coefficient related to catchment flood Δ_2.

References

Archer, D.R., Leesch, F., Harwood, K., 2007. Learning from the extreme River Tyne flood in January 2005. Water Environ. J. 21 (2), 133–141.

Ayral, P.A., 2005. Contribution à la spatialisation du modèle opérationnel de prévision des crues éclair ALHTAÏR. Approches spatiale & expérimentale—Application au bassin versant du Gardon d'Anduze.Université de Provence, Alès, France.

Bechtold, P., Bazile, E., 2001. The 12–13 November 1999 flash flood in southern France. Atmos. Res. 56 (1–4), 171–189.

Borga, M., Gaume, E., Creutin, J.D., Marchi, L., 2008. Surveying flash floods: gauging the ungauged extremes. Hydrol. Process. 22 (18), 3883–3885.

Bras, R.L., 1990. An Introduction to Hydrologic Science. Addison-Wesley Publishing Company (643 pp.).

Braud, I., et al., 2010. The use of distributed hydrological models for the Gard 2002 flash flood event: analysis of associated hydrological processes. J. Hydrol. 394 (1–2), 162–181.

Cohuet, J.B., Romero, R., Homar, V., Ducrocq, V., Ramis, C., 2011. Initiation of a severe thunderstorm over the Mediterranean Sea. Atmos. Res. 100, 603–620.

Costa, J.E., 1987. Hydraulics and basin morphometry of the largest flash floods in the conterminous United States. J. Hydrol. 93 (3–4), 313–338.

Creutin, J.D., Borga, M., Lutoff, C., Scolobig, A., Ruin, I., Créton-Cazanave, L., 2009. Catchment dynamics and social response during flash floods: the potential of radar rainfall monitoring for warning procedures. Meteorol. Appl. 16 (1), 115–125.

Davolio, S., Buzzi, A., Malguzzi, P., 2009. Orographic triggering of long lived convection in three dimensions. Meteorog. Atmos. Phys. 103 (1), 35–44.

Delrieu, G., Ducrocq, V., Gaume, E., Nicol, J., Payrastre, O., Yates, E., Kirstetter, P.-E., Andrieu, H., Ayral, P.-A., Bouvier, C., Creutin, J.-D., Livet, M., Anquetin, S., Lang, M., Neppel, L., Obled, C., Parent-du-Châtelet, J., Saulnier, G.-M., Walpersdorf, A., Wobrock, W., 2005. The catastrophic flash-flood event of 8–9 September 2002 in the Gard Region, France: a first case study for the Cévennes–Vivarais Mediterranean Hydrometeorological Observatory. J. Hydrometeorol. 6 (1), 34–52.

Dingman, S.L., 2002. Physical hydrology. Prentice Hall, NJ, USA.

Furey, P.R., Gupta, V.K., 2005. Effects of excess rainfall on the temporal variability of observed peak-discharge power laws. Adv. Water Resour. 28 (11), 1240–1253.

Gaál, L., et al., 2012. Flood timescales: understanding the interplay of climate and catchment processes through comparative hydrology. Water Resour. Res. 48 (4), W04511. http://dx.doi.org/10.1029/2011WR011509.

Gaume, E., Livet, M., Desbordes, M., Villeneuve, J.-P., 2004. Hydrological analysis of the river Aude, France, flash flood on 12 and 13 November 1999. J. Hydrol. 286 (1–4), 135–154.

Gaume, E., Gaume, E., Bain, V., Bernardara, P., Newinger, O., Barbuc, M., Bateman, A., Blaskovicová, L., Blöschl, G., Borga, M., Dumitrescu, A., Daliakopoulos, I., Garcia, J., Irimescu, A., Kohnova, S., Koutroulis, A., Marchi, L., Matreata, S., Medina, V., Preciso, E., Sempere-Torres, D., Stancalie, G., Szolgay, J., Tsanis, I., Velasco, D., Viglione, A., 2009. A compilation of data on European flash floods. J. Hydrol. 367 (1–2), 70–78.

Gupta, V.K., Castro, S.L., Over, T.M., 1996. On scaling exponents of spatial peak flows from rainfall and river network geometry. J. Hydrol. 187 (1–2), 81–104.

Habets, F., et al., 2008. The SAFRAN-ISBA-MODCOU hydrometeorological model applied over France. J. Geophys. Res. 113 (D06113).

Herschy, R.W., 2002. The world's maximum observed floods. Flow Meas. Instrum. 13 (5–6), 231–235.

Lajournade, C., Beaufrère, C., Lalanne-Berdouticq, G., Martignac, F., 1998. The Biescas disaster, August 7th 1996; geomorphic and hydraulic reconstruction of the rio Aras flood (Aragon, Spain).

Langbein, W.B., 1947. Topographic Characteristics of Drainage Basins. U.S. Geological Survey Water Supply, Paper 968-C, Washington, D.C. , pp. 125–155.

Le Lay, M., Saulnier, G.-M., 2007. Exploring the signature of climate and landscape spatial variabilities in flash flood events: case of the 8–9 September 2002 Cévennes-Vivarais catastrophic event. Geophys. Res. Lett. 34 (L13401). http://dx.doi.org/10.1029/2007GL029746.

Llasat, M.-C., Barriendos, M., Barrera, A., Rigo, T., 2005. Floods in Catalonia (NE Spain) since the 14th century. climatological and meteorological aspects from historical documentary sources and old instrumental records. J. Hydrol. 313 (1–2), 32–47.

Llasat, M.C., et al., 2010. High-impact floods and flash floods in Mediterranean countries: the FLASH preliminary database. Adv. Geosci. 23, 47–55.

Manus, C., et al., 2009. A modeling approach to assess the hydrological response of small Mediterranean catchments to the variability of soil characteristics in a context of extreme events. Hydrol. Earth Syst. Sci. 13 (2), 79–97.

Marchi, L., Borga, M., Preciso, E., Gaume, E., 2010. Characterisation of selected extreme flash floods in Europe and implications for flood risk management. J. Hydrol. 394 (1–2), 118–133.

Molinié, G., Ceresetti, D., Anquetin, S., Creutin, J.D., Boudevillain, B., 2011. Rainfall regime of a Mountainous Mediterranean Region: statistical analysis at short time steps. J. Appl. Meteorol. Climatol. 51 (3), 429–448.

Norbiato, D., Borga, M., Sangati, M., Zanon, F., 2007. Regional frequency analysis of extreme precipitation in the eastern Italian Alps and the August 29, 2003 flash flood. J. Hydrol. 345 (3–4), 149–166.

Nou, A., Nou, A., Pistre, S., Borrell, V., Batiot-Guilhe, C., Bakalowicz, M., Andreo, B., Carrasco, F., Durán, J.J., LaMoreaux, J.W., 2011. Evidence of an Early Phreatic and Confined Karst Phase in Minervois, South of France. Advances in Research in Karst Media, pp. 63–68.

Nuissier, O., Ducrocq, V., Ricard, D., Lebeaupin, C., Anquetin, S., 2008. A numerical study of three catastrophic precipitating events over southern France. I: Numerical framework and synoptic ingredients. Q. J. R. Meteorol. Soc. 134 (630), 111–130.

O'Connor, J.E., Costa, J.E., 2004. Spatial distribution of the largest rainfall-runoff floods from basins between 2.6 and 26,000 km2 in the United States and Puerto Rico. Water Resour. Res. 40 (1), W01107. http://dx.doi.org/10.1029/2003WR002247.

Orlanski, I., 1975. A rational subdivision of scales for atmospheric processes. Bull. Amer. Meteor. Soc. 56, 527–530.

Parajka, J., et al., 2010. Seasonal characteristics of flood regimes across the Alpine–Carpathian range. J. Hydrol. 394 (1–2), 78–89.

Riesco Martín, J., Mora García, M., De Pablo Dávila, F., Rivas Soriano, L., 2013. Severe rainfall events over the western Mediterranean Sea: a case study. Atmos. Res. 127, 47–63.

Robbez-Masson, J.-M., Mazzoni, C., Vallejo, S., Ernesty, D., Falipou, P., 2002. A regional multimedia soil and landscape database on the web in order to help use and teaching of soil data.

Robinson, J.S., Sivapalan, M., 1997. An investigation into the physical causes of scaling and heterogeneity of regional flood frequency. Water Resour. Res. 33 (5), 1045–1059.

Roux, H., et al., 2011. A physically-based parsimonious hydrological model for flash floods in Mediterranean catchment. Nat. Hazards Earth Syst. Sci. 161 (Special Issue), 2567–2582.

Sangati, M., Borga, M., Rabuffetti, D., Bechini, R., 2009. Influence of rainfall and soil properties spatial aggregation on extreme flash flood response modelling: an evaluation based on the Sesia river basin, North Western Italy. Adv. Water Resour. 32 (7), 1090–1106.

Smith, M.B., et al., 2004. Runoff response to spatial variability in precipitation: an analysis of observed data. J. Hydrol. 298 (1–4), 267–286.

Tabary, P., 2007. The New French Operational Radar Rainfall Product. Part I: Methodology. Weather Forecast. 22, 393–408.

Tabary, P., Desplats, J., Do Khac, K., Eideliman, F., Gueguen, C., Heinrich, J.C., 2007. The new French operational radar rainfall product. Part II: validation. Weather Forecast. 22, 409–427.

Tallaksen, L.M., 1995. A review of baseflow recession analysis. J. Hydrol. 165 (1–4), 349–370.

Tarolli, P., Borga, M., Morin, E., Delrieu, G., 2012. Analysis o flash flood regimes in the North-Western and South-Eastern Mediterranean regions. Nat. Hazards Earth Syst. Sci. 12, 1255–1265.

Tramblay, Y., Bouvier, C., Ayral, P.A., Marchandise, A., 2011a. Impact of rainfall spatial distribution on rainfall-runoff modelling efficiency and initial soil moisture conditions estimation. Nat. Hazards Earth Syst. Sci. 11 (1), 157–170.

Tramblay, Y., Neppel, L., Carreau, J., 2011b. Brief communication: climatic covariates for the frequency analysis of heavy rainfall in the Mediterranean region. Nat. Hazards Earth Syst. Sci. 11, 2463–2468.

Viglione, A., et al., 2010. Quantifying space-time dynamics of flood event types. J. Hydrol. 394 (1–2), 213–229 (dedicated to Mediterranean flash-floods. Journal of Hydrology, 394(1–2): 256–266).

Woods, R., Sivapalan, M., 1999. A synthesis of space-time variability in storm response: rainfall, runoff generation, and routing. Water Resour. Res. 35 (8), 2469–2485.

Zoccatelli, D., Borga, M., Zanon, F., Antonescu, B., Stancalie, G., 2010. Which rainfall spatial information for flash flood response modelling? A numerical investigation based on data from the Carpathian range, Romania. J. Hydrol. 394 (1–2), 148–161.

Zoccatelli, D., Borga, M., Viglione, A., Chirico, G.B., Blöschl, G., 2011. Spatial moments of catchment rainfall: rainfall spatial organisation, basin morphology, and flood response. Hydrol. Earth Syst. Sci. 15, 3767–3783.